Optical pulse repetition rate multiplication based on series-coupled double-ring resonator

Xiaowei Dong,* Mengzhen Xu, and Qiangqiang Zhang

College of Information Engineering, North China University of Technology, Beijing 100144, China
*Corresponding author: way7803@163.com

In this paper, optical pulse repetition rate multiplication based on a series-coupled double-ring resonator is proposed. First, the spectral characteristic of the series-coupled double-ring resonator is simulated and the optimum coupling coefficients to achieve a periodic flat-top passband are obtained. Then, high-quality pulse repetition rate multiplication is realized by periodically filtering out spectral lines of the input pulse train. Different multiplication factors $N = 2, 3, 4, 5$ can be obtained by adjusting the ring radii. In addition, compared with a single-ring resonator, the multiplied output pulse train by a series-coupled double-ring resonator exhibits much better power uniformity. © 2016 Chinese Laser Press

    OCIS codes: (130.3120) Integrated optics devices; (230.4555) Coupled resonators; (230.7408) Wavelength filtering devices.
    http://dx.doi.org/10.1364/PRJ.4.000061

1. INTRODUCTION

With the recent development of ultrahigh-speed optical communication systems, techniques for generating and processing high repetition rate optical pulse trains are attracting considerable interest [1]. Since conventional mode-locking or direct-modulating methods are hard to operate at such ultrahigh speed, optical pulse repetition rate multiplication (PRRM) becomes necessary [2]. Most PRRM schemes are based on periodically changing the amplitude and/or phase of the input pulse spectrum. For example, by spectral amplitude filtering, a double-passing Fabry–Perot filter [3], an array waveguide grating [4], and a lattice-form Mach–Zehnder interferometer [5] have been used for generating high repetition rate optical pulse trains. For phase-filtering-based PRRM, chirped-fiber-Bragg gratings [6] have been employed to implement the fractional temporal Talbot effect. Due to the merits of small size and compatibility with the integration process, ring-resonator-based optical PRRM exhibits better applicable prospects. In Ref. [7], optical pulse trains are generated by using a multiple-microring-based time interleaved architecture. In Refs. [8,9], doubling and quadrupling PRRM are obtained by microring-induced beating resonance. In Ref. [10], PRRM and shaping are achieved by ring resonator arrays. However, device fabrication and stability become more difficult as the number of ring resonators increases. Therefore, in this paper, by simulating the spectral characteristic of the series-coupled double-ring resonator, we propose a much more compact optical PRRM with better power uniformity.

2. THEORETICAL BACKGROUND

Figure 1(a) is a typical configuration of a series-coupled double-ring resonator. The transfer function can be obtained by dividing the series-coupled double-ring resonator into three directional couplers (coupling coefficients are K_0, K_1, and

K_2) and two uncoupled half-rings (ring radii are R_1 and R_2, respectively), as shown in Figs. 1(b) and 1(c).

Based on the transfer matrix method, the transfer function of a series-coupled double-ring resonator can be obtained as [11]

$$G = -j \left\{ \prod_{k=1,2} \begin{bmatrix} \frac{\tau_k^{1/2} \cdot e^{j\beta \cdot \pi R_k}}{K_k} & -\frac{\tau_k^{-1/2} \cdot e^{-j\beta \cdot \pi R_k} \cdot T_k}{K_k} \\ \frac{\tau_k^{1/2} \cdot e^{j\beta \cdot \pi R_k} \cdot T_k}{K_k} & -\frac{\tau_k^{-1/2} \cdot e^{-j\beta \cdot \pi R_k}}{K_k} \end{bmatrix} \right\} \cdot \begin{bmatrix} \frac{1}{K_0} & -\frac{T_0}{K_0} \\ \frac{T_0}{K_0} & -\frac{1}{K_0} \end{bmatrix}, \quad (1)$$

where $\beta = 2\pi \cdot n_{\mathrm{eff}}/\lambda$ is the propagating constant, n_{eff} is the effective refractive index, λ is the wavelength, $\tau_k = \exp(-\alpha \cdot 2\pi R_k)$ is the waveguide normalized loss, and T_k and K_k are the normalized transferring coefficient and coupling coefficient, which have the relationship $T_k^2 + K_k^2 = 1$.

By assuming no input signal at port 3 ($E_3 = 0$) and defining one-round phase within the ring as $\phi_{1,2} = (2\pi \cdot n_{\mathrm{eff}}/\lambda) \cdot 2\pi R_{1,2}$, the spectral responses at drop port $D(\lambda)$ can be obtained as

$$D(\lambda) = \frac{E_4}{E_1}$$
$$= \frac{jK_1 K_2 K_3 \tau_1^{1/2} \tau_2^{1/2} e^{j(\phi_1+\phi_2)/2}}{1 - (T_1 T_2 \tau_1 e^{j\phi_1} + T_2 T_3 \tau_2 e^{j\phi_2}) + T_1 T_3 \tau_1 \tau_2 e^{j(\phi_1+\phi_2)}}. \quad (2)$$

Due to the resonant characteristic, $D(\lambda)$ is periodic with respect to the inverse of wavelength. Defining $\mathrm{FSR} = \lambda_{m+1} - \lambda_m$ as the periodic resonant spacing and using the inverse Fourier transform (F^{-1}), the temporal domain impulse response of $D(t)$ is discrete-time, as shown by [5]

$$D(t) = \sum_{p=-\infty}^{\infty} F^{-1}(D(\lambda))|_{t=p/\mathrm{FSR}} \cdot \delta(t - p/\mathrm{FSR}). \quad (3)$$

When a periodic input pulse train $a_{\mathrm{in}}(t) = \sum_{q=-\infty}^{\infty} a_0(t - qT)$ (where $a_0(t)$ represents the complex envelope of an individual pulse and T is the temporal period) is injected into port 1, the
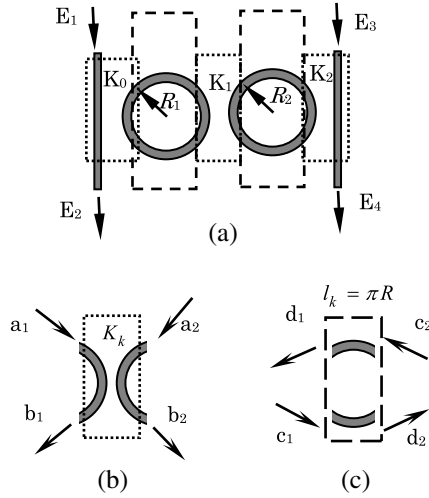
Fig. 1.   (a) Series-coupled double-ring resonator, (b) directional coupler, and (c) uncoupled half-ring.

output is the convolution ($\otimes$) between the input $a_{in}(t)$ and the impulse response of $D(t)$, as shown by

$$O(t) = a_{in}(t) \otimes D(t)$$
$$= \sum_{p=-\infty}^{\infty} \sum_{q=-\infty}^{\infty} F^{-1}(D(\omega))|_{t=qT+p/\text{FSR}} \cdot a_{in}(t - qT - p/\text{FSR}).$$
$$(4)$$

When the periodic resonant spacing (FSR) of the series-coupled double-ring resonator and the temporal period T of the input pulse train meet the condition $T \cdot \text{FSR} = N$, the repetition rate of the output pulse train can be multiplied by a factor of N if the input pulsewidth is sufficiently narrow [12].

3. ANALYSES AND DISCUSSION

In the following numerical analyses, we examine optical PRRM using the aforementioned series-coupled double-ring resonator. Due to the high refractive index contrast of silicon-on-insulator (SOI) technology, a wavelength-scale microring resonator can be fabricated with very small bend loss. By setting the width and height of the top silicon waveguides as 500 and 230 nm, respectively, and assuming polymer SU8 as the top cladding layer, the group index is calculated approximately to be 3.901 at 1550 nm wavelength [13].

First, the spectral responses of the series-coupled double-ring resonator are studied. When both the rings have the same radius R, similarly to the single-ring resonator, the series-coupled double-ring exhibits a periodic resonant spacing FSR, as shown in Fig. 2(a). However, different from the Lorentzian spectral response of the single-ring resonator, the resonant passband within each period of the series-coupled double-ring resonator is divided into two narrower subresonant passbands, whose spacing and shaping depend on the coupling coefficients. As demonstrated in Figs. 2(b) and 2(c), when the internal coupling coefficients of the adjacent rings K_1 increase, the subresonant spacing expands, whereas, when the external coupling coefficients between the rings and the input/output waveguides (K_0 and K_2) increase, the subresonant passbands will recombine and evolve into one broader flat-top passband if the following two conditions are satisfied [14]: $K_0 = K_2$ and $K_1 = K_0^2/(2 - K_0^2) \approx K_0^2/2$.
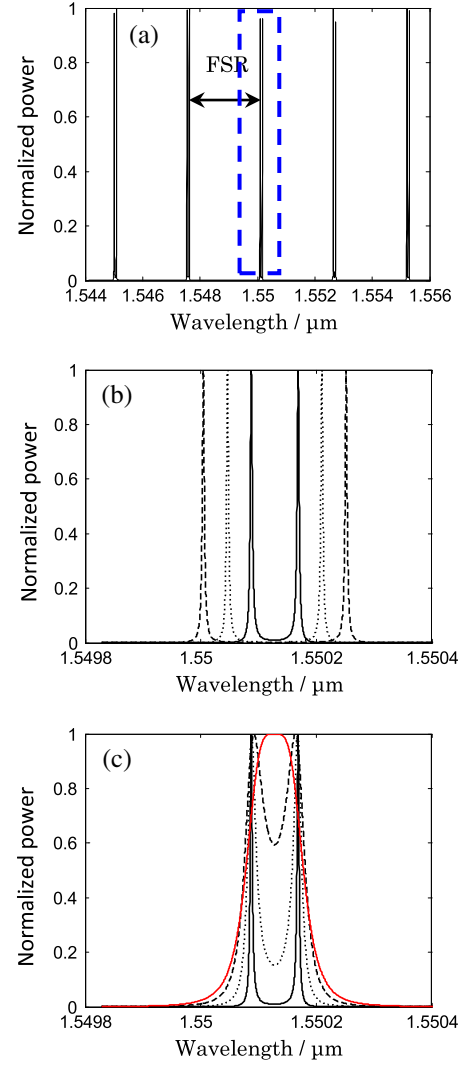

Fig. 2.   (a) Spectral responses of series-coupled double-ring resonator. (b),(c) Influence of coupling coefficients on the resonant passband within the zoom-in area of (a). (b) Internal coupling coefficients $K_1 = 0.1$ (solid), 0.2 (dotted), and 0.3 (dashed) when $K_0 = K_2 = 0.1$. (c) External coupling coefficients $K_0 = K_2 = 0.1$ (solid), 0.2 (dotted), 0.3 (dashed), and 0.426 (red) when $K_1 = 0.1$.

Next, PRRM is investigated by employing a series-coupled double-ring resonator with a flat-top resonant passband. We assume that a 10 GHz Gaussian-pulse train is input and the full width at half-maximum (FWHM) of each pulse is 1 ps, which is narrow enough to avoid interfering with each other. When the radii of the series-coupled double-ring resonator are set to be 612 μm, its periodic resonant spacing FSR equals twice that of the spectral comb of the input pulse train, so that every other spectral line will be filtered out, which results in the output spectral line spacing being doubled and repetition rate multiplication with a factor of 2 being achieved, as shown in Fig. 3. According to the law of conservation of energy, only half of the incident power remains for ×2 repetition rate multiplication. In addition, due to the fabrication difficulty, it is hard to set the resonator radius accurately. Figure 3(e) shows the output pulse trains for resonator radii with ±100 and ±200 nm fabrication deviation. As the resonator radii deviating from the ideal values increase, the output pulse

Dong *et al.*
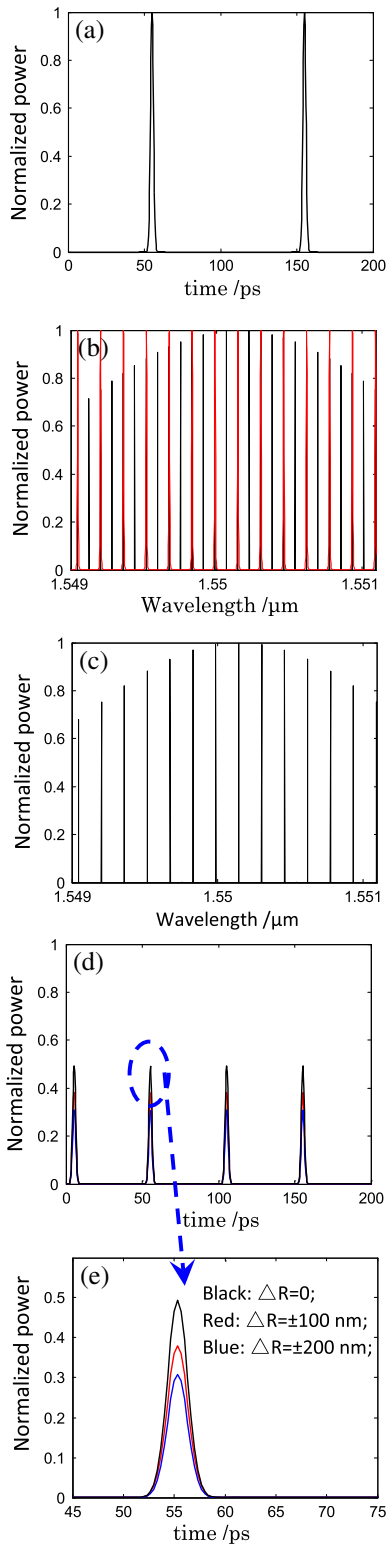
Vol. 4, No. 2 / April 2016 / Photon. Res.   63

Fig. 3. (a) Input pulse train of 10 GHz. (b) Optical spectra of input pulse train (black line) and series-coupled double-ring resonator (red line). (c) Optical spectrum of output pulse train. (d) Output pulse train with multiplication factor 2. (e) Single pulse with different resonator radii deviation.

trains decrease and system power loss deteriorates. Although the power loss can be compensated by adding an optical amplifier, we suggest that the fabrication deviation should
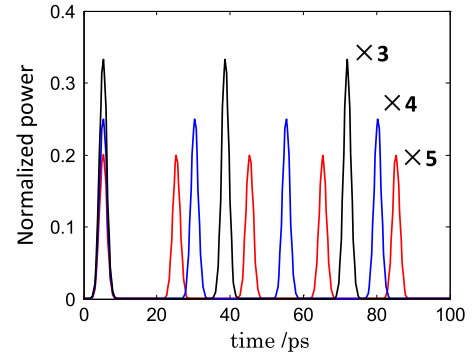

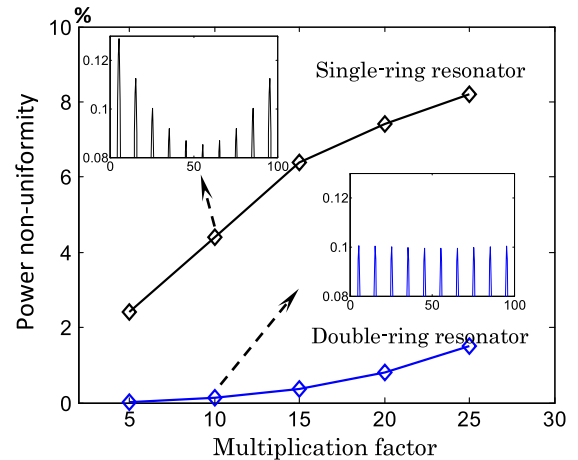Fig. 4. Output pulse trains with multiplication factors 3 (black), 4 (blue), and 5 (red).

Fig. 5. Comparison of power nonuniformity. Inset: output pulse trains by single-ring and double-ring resonator with factor 10.

be kept as small as possible in order to obtain better PRRM performance. Compared with other reported systems [3,4], series-coupled double-ring resonators have the advantage that the shape of each individual output pulse remains unchanged from the original input pulses.

Since the periodic resonant spacing FSR is approximately inversely proportional to the ring radii [15], larger FSR and higher PRRM can be achieved by using a resonator with smaller size. As shown in Fig. 4, output pulse trains with multiplication factors of 3, 4, and 5 are obtained by employing series-coupled double-ring resonators with radii of 408, 306, and 245 μm, respectively. To judge the quality of multiplied pulses, the power nonuniformity of the output pulse train is calculated as [16] $\Delta = \text{var}(O(t))/\text{mean}(O(t)) \times 100\%$. It is obvious that the power uniformity is much better for the series-coupled double-ring resonator compared with the single-ring resonator as the multiplication factor increases, as demonstrated in Fig. 5. This is because of the broader and flatter passband characteristic of the series-coupled double-ring resonator, which allows a higher tolerance to external noise and fabrication errors.

4. CONCLUSIONS

In this paper, based on the transfer matrix method, the spectral characteristic of the series-coupled double-ring resonator is simulated. The influence of the internal and external

coupling coefficients on the subresonant passband is analyzed, and the optimum coupling coefficients to achieve the flat-top passband filtering response are obtained. Then, high-quality PRRM is realized by a series-coupled double-ring resonator to periodically filter out the spectral lines of the input pulse train. In addition, by adjusting ring radii, output pulse trains with different multiplication factors are achieved, which exhibit much better power uniformity compared with the single-ring resonator.

ACKNOWLEDGMENT

REFERENCES

1. M. P. Fok, W. W. Tang, and C. Shu, "Higher order repetition rate multiplication for multi-wavelength pulsed source," IEEE Photon. Technol. Lett. **18**, 466–468 (2006).
2. C. K. Chan and L.-K. Chen, "Theoretical analysis of high-repetition rate optical pulse multiplication using fiber-coupler loop configuration," IEEE Photon. Technol. Lett. **7**, 1145–1147 (1995).
3. K. Yiannopoulos, K. Vyrsokinos, E. Kehayas, N. Pleros, K. Vlachos, H. Avramopoulos, and G. Guekos, "Rate multiplication by double-passing Fabry–Perot filtering," IEEE Photon. Technol. Lett. **15**, 1294–1296 (2003).
4. D. S. Seo, D. E. Leaird, A. M. Weiner, S. Kamei, M. Ishii, A. Sugita, and K. Okamoto, "Continuous 500 GHz pulse train generation by repetition-rate multiplication using arrayed waveguide grating," Electron. Lett. **39**, 1138–1140 (2003).
5. B. Xia and L. R. Chen, "A direct temporal domain approach for pulse-repetition rate multiplication with arbitrary envelope shaping," IEEE J. Sel. Top. Quantum Electron. **11**, 165–172 (2005).
6. J. Azana and M. A. Muriel, "Temporal self-imaging effects: theory and application for multiplying pulse repetition rates," IEEE J. Sel. Top. Quantum Electron. **7**, 728–744 (2001).
7. S. Wang, B. Ciftcioglu, and H. Wu, "Microring-based optical pulse-train generator," Opt. Express **18**, 19314–19323 (2010).
8. L. Xu, C. Li, H. K. Tsang, and C. W. Chow, "Optical frequency doubling for multichannel radio-over-fiber system based on integrated phase modulator and silicon coupled microring notch filter," Electron. Lett. **45**, 697–698 (2009).
9. L. Xu, C. Li, C. W. Chow, and H. K. Tsang, "Optical mm-wave signal generation by frequency quadrupling using an optical modulator and silicon microresonator filter," IEEE Photon. Technol. Lett. **21**, 1211–1213 (2009).
10. B. Xia and L. R. Chen, "Ring resonator arrays for pulse repetition rate multiplication and shaping," IEEE Photon. Technol. Lett. **18**, 1999–2001 (2006).
11. B. Xia and L. R. Chen, "Arbitrary optical waveform generation using 2D ring resonator arrays," Opt. Express **14**, 6619–6627 (2006).
12. M. Pu, H. Ji, L. H. Frandsen, M. Galili, L. K. Oxenlowe, and J. M. Hvam, "High-Q microring resonator with narrow free spectral range for pulse repetition rate multiplication," in *Conference on Lasers and Electro-Optics* (2009), paper CThBB7.
13. M. Xiong, O. Ozolins, Y. Ding, B. Huang, Y. An, H. Ou, C. Peucheret, and X. Zhang, "Simultaneous RZ-OOK to NRZ-OOK and RZ DPSK to NRZ-DPSK format conversion in silicon micro-ring resonator," Opt. Express **20**, 27263–27272 (2012).
14. D. Xiaowei, P. Li, and J. Shuisheng, "Characteristic analyses of series-coupled multiple-ring resonator filter," Acta Opt. Sin. **26**, 207–211 (2006).
15. O. Schwelb, "Transmission, group delay, and dispersion in single-ring optical resonators and add-drop filters—a tutorial overview," J. Lightwave Technol. **22**, 1380–1394 (2004).
16. M. A. Preciado and M. A. Muriel, "All-pass optical structures for repetition rate multiplication," Opt. Express **16**, 11162–11168 (2008).